Journal of Mining and Environment (JME) Vol. 18, No. 4, 2026, 1409-1427

Shahrood University of Technology

Journal of Mining and Environment (JME)

Journal homepage: www.jme.shahroodut.ac.ir

Iranian Society of Mining Engineering (IRSME)

Investigating the Relationship between Cerchar Abrasivity Index with Physico-mechanical and Petrographic Properties of Granitic Building Stones

Sina Ghavami[1], Ebrahim Ghasemi[1*], Mohammad Hossein Kadkhodaei[1], and Ali Farhadian[2]

1. Department of Mining Engineering, Isfahan University of Technology, Isfahan, Iran
2. Assistant Professor, Mining Group, Faculty of Eng., University of Jiroft, Kerman, Iran

Article Info

Received 27 May 2025
Received in Revised form 1 July 2025
Accepted 27 July 2025
Published online 27 July 2025

DOI: 10.22044/jme.2025.16303.3167

Keywords

Cerchar abrasivity index (CAI)
Granitic building stones
Petrographic properties
Physico-mechanical properties
Diamond segment wear (SW)
Statistical analysis

Abstract

Consumption of cutting and polishing tools is a critical economical parameter during quarrying and processing of granitic building stones, which is highly affected by stone abrasivity. So, estimation of abrasivity for these stones is a very important issue. There are several methods to determine the stone abrasivity. One of the most commonly used methods is Cerchar abrasivity index (CAI). This study mainly focuses on investigating the relationship between CAI with petrographic and physico-mechanical properties of granitic building stones. For this purpose, 14 different types of commercial granitic building stones, collected from different regions of Iran, were subjected to laboratory investigations and the effect of the petrographic and physico-mechanical properties of these stones on CAI was examined using simple and multiple regression analysis. Meaningful and reasonable relationships were observed. According to the obtained results, equivalent quartz content (EQC) of granitic building stones was found to be the most effective parameter on CAI. Using linear and nonlinear regression analysis, two empirical correlations for CAI prediction based on EQC were developed. The results showed that both linear and nonlinear correlations have high performance with determination coefficients (R2) of 0.876 and 0.882, respectively. These correlations can determine the CAI with acceptable error, with root mean square error (RMSE) and mean absolute error (MAE) values of 0.135 and 0.105, respectively. Furthermore, the relationship between the diamond segment wear (SW) and CAI was investigated for the studied stones. The results showed that SW is directly related to the CAI, and there is a strong linear correlation between these two parameters with R2 of 0.787. The proposed correlation can be applied for fast prediction of cutting tool wear for practical applications in building stone processing plants with circular sawing machine, which can lead to enhanced cutting efficiency and productivity.

1. Introduction

Granitic building stones are widely used as one of the main materials in buildings' interior and exterior facing due to their excellent resistance and aesthetic characteristics. Since quartz is the main existing mineral in these stones, they are classified as hard and abrasive stones [1]. Stone abrasivity (SA) is defined as the ability of stone to wear down a tool [2]. Consumption (wear) of cutting and polishing tools during quarrying and processing of these stones is very high due to high abrasivity, which results in more costs. So, it is essential to evaluate abrasivity of these stones. During recent years, various laboratory tests (applicable in special and general cases) have been developed to evaluate SA. One of the most commonly used tests is the Cerchar abrasivity test. This test is a simple, fast and cost-effective method to determine an index called Cerchar abrasivity index (CAI) for evaluating abrasivity of stones, which was originally introduced in the 1970s by the Center

Corresponding author: e_ghasemi@iut.ac.ir (E. Ghasemi)

d'Etudes et Recherches des Charbonages (Cerchar) de France for coal mining industry [3]. Three standards exist for performing this test: ASTM D7625-10, the French standard NF P 94-430-1, and ISRM [4]. Furthermore, there are two basic designs for test apparatus to perform this test: the original design (developed at the Cerchar center) and the modified design (developed by West) [5]. The CAI is obtained by scratching the tip of a sharp steel stylus, with Rockwell Hardness C (HRC) 54-56 and tensile strength of 200 kg/mm2, on a fresh (rough) surface of stone. This stylus has a sharp conical tip with a cone angle of 90 degrees, and a static force of 70 N is loaded on it. This stylus is scratched at 10 mm from the sample's surface at a rate of 1 mm/s; after scratching, the wear flat on the stylus tip is measured under a microscope to an accuracy of 0.01 mm. The wear flat number is then multiplied by 10, and defined as the CAI which indicates the SA. According to the CAI value, rock abrasivity is classified into seven categories: 1) Extremely low (CAI: 0.1-0.4), 2) Very low (CAI: 0.5-0.9), 3) Low (CAI: 1-1.9), 4) Medium (CAI: 2-2.9), 5) High (CAI: 3-3.9), 6) Very high (CAI: 4-4.9), and 7) Extremely high (CAI≥5) [6].

Many parameters affect the amount of CAI. These parameters can be divided into two categories [4,7]: (1) testing condition-based parameters such as stylus metallurgy and hardness, testing apparatus, testing velocity and distance, testing repetition, measurement of stylus wear, surface condition of stone. and (2) geological and geotechnical-based parameters which are related to grain size and shape, mineral composition and content, quartz content and its equivalence, as well as rock properties including hardness, strength and etc. After development of Cerchar abrasivity test, many researchers have studied the effects of geological and geotechnical-based parameters on CAI, which is also the focus of the present study. For example, Suana and Peters [8] and West [9] have mentioned that the quartz content (Q) of the stone is a significant affecting parameter on CAI. Al-Ameen and Waller reported that CAI test is largely influenced by the rock strength [10]. Plinninger et al. studied 109 stone samples and showed that combination of the Young's modulus (E) and the equivalent quartz content (EQC) of a stone sample has a fair correlation with CAI [11]. Lassnig et al. indicated that mineral grain size has no obvious influence on the CAI when its value varies between 50 μm and 100 μm [12]. Yaralı et al. investigated the relations between the CAI and petrographic properties of coal measures rocks in the Zonguldak Coal Basin, Turkey. They found that there is a good linear relationship between the CAI values of rocks and their degree of cementing, quartz content, EQC, and quartz grain size [13]. Khandelwal and Ranjith investigated the relationship between P-wave velocity (Vp) and CAI based on two samples of igneous stones, eight samples of sedimentary stones, and three samples of metamorphic stones [14]. Altindag et al. found that the CAI value is related with brittleness and uniaxial compressive strength (UCS) of rocks [15]. Kahraman et al. used CAI for indirect prediction of the E and UCS of Misis Fault Breccia using regression and artificial neural networks analysis [16]. Dipova investigated the relationship between CAI and the strength properties of weak limestones in Texas tunnel [17]. Deliormanlı examined 15 marble stones and used simple and multiple regression analysis (SRA and MRA) to determine the relation between the CAI value, wear properties, and strength of these stones [18]. Tripathy et al. investigated the relationship between CAI of different rock types and UCS, point load strength index (PLI), Vp, and E using artificial neural network and MRA. They found that artificial neural network has a high accuracy in predicting the CAI [19]. Er and Tuğrul investigated the correlation between the chemical, petrographic and physico-mechanical properties with CAI based on 12 Turkish granitic stones using the SRA [20,21]. He et al. studied the correlation between CAI with the mechanical, petrographic and microstructure properties. They found that the combination of mechanical parameters, microstructure coefficient and EQC leads to better correlations using logarithmic regression [22]. Majeed and Bakar evaluated the correlations of CAI with Schimazek's F value (F), rock abrasivity index (RAI), petrographic and physico-mechanical properties of 46 rock units in Pakistan [23]. Moradizadeh et al. studied the relation between the CAI and EQC, and several geomechanical properties, such as the PLI, slake durability index, and percentage of water absorption of 36 different stone samples [24]. Bakar et al. studied the dependency of CAI on the water content of stones and found that the CAI value in saturated stone is about 79% of that in dry stone [25]. Ko et al. investigated the correlation between geomechanical properties of metamorphic and igneous stones including Brazilian tensile strength (BTS), Q, UCS, and brittleness index with CAI using SRA and MRA. They found that a single parameter alone is not suitable to predict the value of CAI. Brittleness index and UCS are the more influencing parameters on prediction model for igneous stones and BTS and UCS are the more influencing parameters for metamorphic stones [3]. Ündül and Er examined the effects of the geomechanical and micro-textural properties on the CAI of volcanic stones. They found that Vp is the most important parameter in assessing the CAI values for the studied stones [26]. Capik and Yilmaz examined the relationships between the CAI and some rock properties such as PLI, UCS, BTS, Schmidt rebound hardness (SCH), and EQC using SRA and MRA. The results showed that the developed correlations based on EQC and UCS are better for prediction of CAI [27]. Cheshomi and Moradhaseli investigated the effect of petrographic characteristics on CAI of 18 samples of granitic building stones and developed a new experimental relation between EQC and CAI [28]. Ozdogan et al. analyzed the relation between CAI and three geomechanical properties of igneous, sedimentary, and metamorphic building stones including porosity (P), Shore hardness (SH), and UCS using SRA and MRA. They realized that the CAI value is strongly related to SH [29]. Torrijo et al. investigated the relation between CAI and the chemical compounds and petrographical properties of 73 andesite rocks of the central area of Ecuador. They found that it is possible to make a good estimation of CAI from the plagioclase grain size and/or the content of FeO, SiO2, MgO, CaO, K2O and Na2O compounds [30]. Erarslan analyzed the viability of Cerchar abrasivity test for evaluating the abrasivity of anisotropic stones such as phyllite. He investigated the correlation between EQC, F, RAI and CAI. The obtained results showed that F and RAI values should be considered when determining the abrasivity of anisotropic rocks instead of just using Cerchar abrasivity test [31]. Kadkhodaei and Ghasemi developed a mathematical relation to predict the CAI using gene expression programming (GEP) method based on a database collected from the experimental results available in the literature. The proposed GEP model predicts CAI based on two basic geomechanical properties of rocks, i.e. BTS and RAI [32]. Teymen carried out a series of statistical studies to estimate the basic rock mechanics properties which are difficult to determine and time-consuming with the help of CAI values. The results of his study indicated that there are significant relationships between basic mechanical rock properties and CAI [33]. Garzón-Roca et al. developed several ANN models to estimate CAI values of andesitic rocks from their petrographic properties Using data provided by Torrijo et al. [34]. Zhang et al. examined the relationship between CAI and physico-mechanical properties of 13 groups of rock samples from southwestern China. The results showed that among all the studied parameters, two UCS and EQC are the most important parameters to obtain the CAI [35]. Cheshomi and Moradizadeh proposed new relations between RAI with CAI for granitic building stones. furthermore, they introduced a new parameter, i.e. modified rock abrasivity index (MRAI) to investigate the simultaneous effect of BTS, UCS and EQC on CAI and found a strong relationship between this parameter and CAI [28]. Kwak and Ko used machine learning-based regression methods (including regression tree, support vector regression, k-nearest neighbors, random forest, and artificial neural network) to predict CAI based on petrographic and mechanical properties of 223 rock types [36].

As mentioned before, abrasivity is one of crucial parameters in the quarrying and processing costs of granitic building stones. Despite the importance of this subject, literature review reveals that very limited work has been conducted to evaluate the abrasivity of granitic building stones. In other words, literature review shows a significant gap in comprehensive studies focusing specifically on granitic building stones, particularly in developing predictive models for both CAI and diamond segment wear (SW) tailored to the building stone industry. Thus, the primary purpose of this study is to investigate the correlation between CAI with the petrographic and physico-mechanical properties of granitic building stones. For this purpose, 14 different types of Iranian granitic building stones are subjected to laboratory investigations and the effect of the petrographic and physico-mechanical properties of these stones on CAI is examined using SRA and MRA. Then, new predictive correlations for CAI are developed. The secondary purpose of this study is to develop new correlation for estimating diamond segment wear (SW) during cutting of studied stones using circular sawing machine. For this purpose, the cutting tests are performed on the stones using circular disc sawing machine equipped with diamond segment to determine SW. Then, the relationship between the SW and CAI is investigated.

2. Materials and methods

To do this study, 14 different types of Iranian commercial granite stones were collected from building stone processing plants of Mahmoud

Abad industrial town, Isfahan, Iran. These stones were extracted from the quarries located in eight provinces of Iran (see Figure 1 and Table 1). Commercial granite covers all crystalline and hard igneous rocks with different petrographic and mineralogical properties that capable of taking a good polish [37]. Granite samples were prepared in block form with enough dimensions and brought to the laboratory for testing (physico–mechanical properties tests and petrographic analyses). All of the granite samples were without visible cracks and fractures to avoid the influence of anisotropy on the measurement. It should be noted that the report of some tests on these stones has been presented in previous study conducted by Farhadian et al. [38].

Table 1. Commercial and scientific names of studied stones

Stone No.	Commercial name	Province	Scientific name	Stone code
1	Meshki-Natanz	Isfahan	Diorite	MN
2	Sefid-Natanz	Isfahan	Granodiorite	SN
3	Khorramdarreh	Zanjan	Syenogranite	KH
4	Golpanbehi Nehbandan	South Khorasan	Granite	GN
5	Taybad	Razavi Khorasan	Syenogranite	TY
6	Borujerd	Lorestan	Granite	BO
7	Zahedan	Sistan and Baluchestan	Granite	ZA
8	Ghermez-Yazd	Yazd	Andesite	GY
9	Morvarid-Mashhad	Razavi Khorasan	Granite	MO
10	Shaghayegh Nehbandan	South Khorasan	Monzonite	SN
11	Toosi Astan	South Khorasan	Granite	TA
12	Kerem-porteghali Nehbandan	South Khorasan	Granite	KP
13	Holoee Zanjan	Zanjan	Syenite	HZ
14	Maragheh	East Azerbaijan	Syenogranite	MA

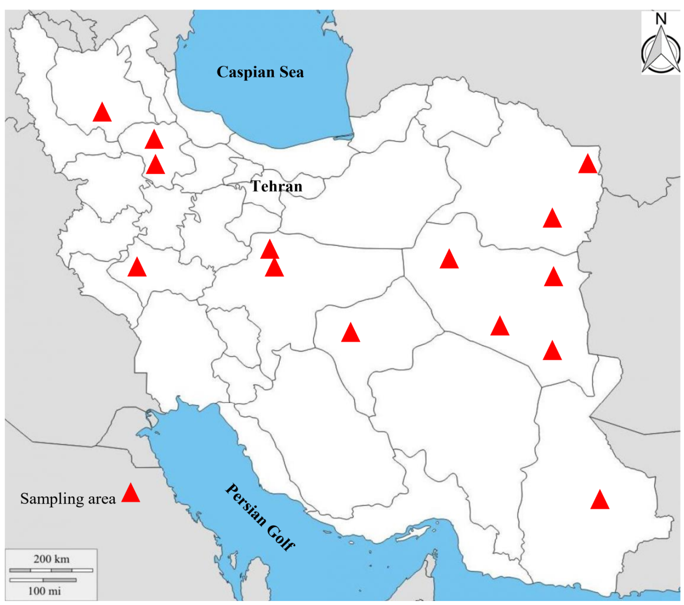

Figure 1. Quarries locations in Iran

2.1. Petrographic analyses

One of the most common methods for determining petrographic properties of stones is to examine thin sections under polarized microscope. Figure 2 shows thin section micrographs of the studied stones. By examining thin section, the mineral compositions and then some of the essential petrographic properties such as the quartz content (Q), ratio of quartz to cleavable minerals (Q/CLV), and cleavable minerals content (CLV) were determined for each stone sample. Table 2 presents mineral compositions of granite samples. As can be seen in Table 2, mineral constituents of the samples are quartz, K-feldspar, plagioclase feldspar, and minor amounts of accessory minerals such as hornblende, biotite, muscovite, amphibole, epidote, opaque, etc. Furthermore, cleavable minerals include plagioclase, K-feldspar, hornblende, biotite, etc [37].

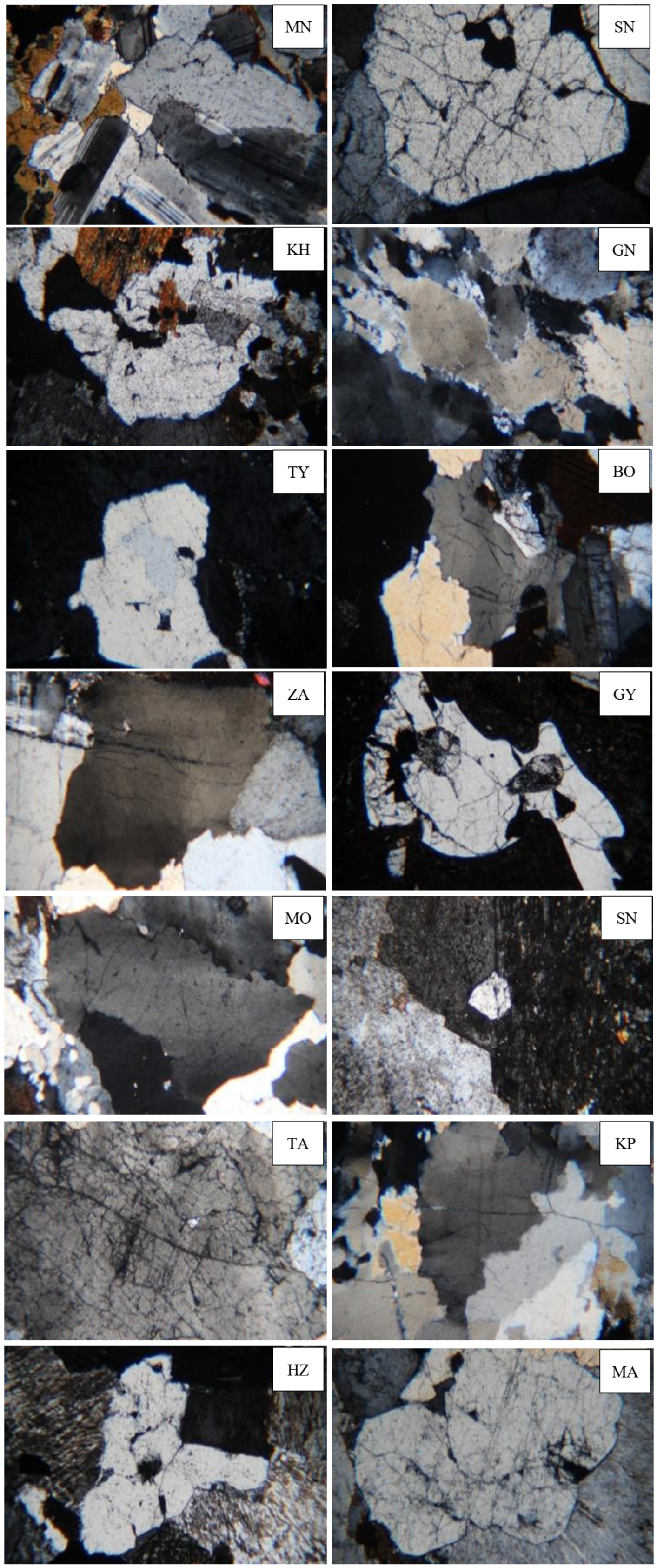

Figure 2. Thin section micrographs of the studied stones

Table 2. Mineral compositions of granite samples

Stone code	Quartz (%)	Plagioclase (%)	K-feldespar (%)	Accessory minerals (%)
MN	10	60	-	30
SN	23	51	5	21
KH	20	15	50	15
GN	28	26	35	11
TY	30	20	45	5
BO	22	38	30	90
ZA	47.5	23	19	10.5
RY	20	15	-	65
MO	23.5	19	43.5	14
SN	19	33.5	36	11.5
TA	40	20	28	12
KP	40	25	30	5
HZ	8	8	75	9
MA	25	16	54	5

Obtained results from thin sections examination can be used to calculate the overall Mohs hardness (MH), EQC, and equivalent grain size (Gs) for each sample. Equation 1 was used to obtain Gs for each stone sample [39]:

$$Gs = S_q \times P_q + S_{kf} \times P_{kf} + S_{pl} \times P_{pl} \quad (1)$$

Where are:

S_q is the mean grain size of quartz,

S_{kf} - the K-feldspar mineral,

S_{pl} - the plagioclase mineral,

P_q - the quartz percentage contents,

P_{kf} - the K-feldspar percentage contents,

P_{pl} - the plagioclase percentage contents.

Due to their relatively low percentage contents and small grain sizes, the accessory minerals were not included in the granite grain size calculations.

EQC of the samples can be calculated by multiplying the percentage of minerals present in the stone with their respective Rosiwal hardness values using Equation 2 [40]:

$$EQC = \sum_{i=1}^{n} P_i \times R_i \quad (2)$$

Where are:

P_i - the percentage content of mineral present in the stone,

R_i - the Rosiwal hardness for the mineral relative to quartz,

n - the number of minerals.

MH of a stone can be determined by combining the Mohs hardness of the individual minerals making up the stone and the mineral percentage using Equation 3 [41]:

$$MH = \sum_{i=1}^{n} M_i \times P_i \quad (3)$$

Where are:

M_i - the Mohs number for the mineral,

P_i - the percentage of mineral present in the stone,

n - the number of minerals.

The obtained values of petrographic properties including Q, CLV, Q/CLV, EQC, Gs, and MH for different types of samples have been presented in Table 3.

2.2. Physico-mechanical properties

In this stage, physical properties including porosity (P), density (D), and P-wave velocity (Vp) and mechanical properties including UCS, BTS, and Schmidt rebound hardness (SCH) were determined for all samples according to standard methods. Table 4 shows the method of determining the physico-mechanical properties of the samples based on the standard methods of each test. The values of physico-mechanical properties of the stones are listed in Table 5.

Table 3. Petrographic properties for samples

Stone code	Q (%)	CLV (%)	Q/CLV	G_s (mm)	EQC (%)	MH
MN	10.0	87.5	0.11	1.32	38.58	5.44
SN	23.0	74.0	0.31	1.58	46.20	5.71
KH	20.0	73.0	0.27	1.71	48.97	5.88
GN	28.0	72.0	0.39	1.55	49.83	5.95
TY	30.0	70.0	0.43	1.93	52.95	6.14
BO	22.0	78.0	0.28	1.78	46.14	5.89
ZA	47.5	52.0	0.91	2.83	62.60	6.12
RY	20.0	78.0	0.26	0.42	41.17	5.79
MO	23.5	76.5	0.31	0.69	45.94	5.78
SN	19.0	79.0	0.24	1.03	47.29	5.94
TA	40.0	58.0	0.69	3.92	57.95	6.04
KP	40.0	60.0	0.67	3.33	59.39	6.23
HZ	8.0	89.0	0.09	2.06	39.75	5.89
MA	25.0	75.0	0.33	2.07	49.70	6.09

Table 4. Determination of physical and mechanical properties of samples based on standard methods

Test	Standard	Description	Reference
Porosity (P) and Density (D)	ISRM	Determined using the saturation and buoyancy method. To determine these properties, at least three samples of each stone types were tested and the average values were considered.	[42]
P-wave velocity (Vp)	ISRM	Vp was determined for each stone type using a Portable Ultrasonic Nondestructive Digital Indicating Tester (PUNDIT Lab+) instrument and two transducers (a transmitter and a receiver) having a frequency of 54 kHz. The direct transmission method was used to measure the P-wave travel times. Also, a coupling gel was applied on the surfaces of the specimens to avoid any air gap between the sample and transducers to maximize the accuracy of transit time measurement. The Vp values were calculated by dividing the sample length and the transit pulse time. The average of three measurements for each stone type was considered as Vp in this study.	[42]
Uniaxial compressive strength (UCS)	ASTM C170	Three cubical-shaped samples from each stone type (with the dimensions of 7 × 7 × 7 cm) were used to determine the UCS values. The stress rate was applied uniformly within the limits of 0.5–1 MPa/s until failure occurred. The average of three measurements were used as UCS in this study.	[43]
Brazilian tensile strength (BTS)	ISRM	To measure the BTS, at least three core samples of each stone type (with the diameter of 54 mm and thickness of 27 mm) were tested according to the standard method, and the average values were considered.	[42]
Schmidt rebound hardness (SCH)	ISRM	The SCH was determined for each stone type using the L-type Schmidt hammer with an impact energy of 0.735 N.m according to the standard method. The hammer was held vertically downwards at stone faces to avoid the necessity for a correction factor. In order to determine the SCH value of the stones, 20 strokes were applied to the smooth surfaces of the block-shaped stones and the average of the highest 10 values was calculated.	[44]

Table 5. Physico-mechanical properties, CAI and SW values for studied stones

Stone code	D (g/cm^3)	P (%)	UCS (MPa)	BTS (MPa)	Vp (m/s)	SCH	CAI	SW (gr)
MN	2.77	0.84	136.10	10.30	4802.00	66.25	3.25	0.285
SN	2.66	1.33	124.80	9.06	4648.33	58.64	3.69	0.258
KH	2.57	1.23	131.94	10.11	5424.00	65.88	3.83	0.264
GN	2.62	1.06	139.94	11.78	5449.33	64.26	3.96	0.402
TY	2.85	1.14	152.20	12.12	5660.00	68.60	4.03	0.441
BO	2.58	1.39	118.30	8.53	4254.00	56.11	3.61	0.300
ZA	2.54	1.58	149.60	11.52	5650.00	70.00	4.68	0.535
RY	2.56	2.09	127.50	8.82	5000.00	58.00	3.25	0.244
MO	2.65	1.06	137.50	10.30	4709.75	57.56	3.79	0.337
SN	2.61	1.10	143.27	10.36	5175.00	63.16	3.96	0.396
TA	2.61	1.41	147.23	12.46	5500.00	64.26	4.42	0.471
KP	2.78	0.93	149.00	11.78	5700.00	68.38	4.05	0.395
HZ	2.56	3.26	131.80	10.35	4651.65	56.90	3.46	0.192
MA	2.85	2.03	145.80	11.77	5571.30	66.07	3.83	0.396

2.3. Cerchar abrasivity test

The Cerchar abrasivity test was performed using modified device designed by West with pins of HRC 54-56 (Figure 3). During the test, the specimen is fixed with a vise, the steel stylus is in contact with the surface of the test sample under a static load of 70 N, and the steel stylus is moved at a speed of 1 mm/s over a distance of 10 mm on the stone surface by moving the control handle. The wear flat on the stylus tip, by the high-resolution camera with a magnification of 1000, is photographed (Figure 4a), and the wear flat of the pin tip is obtained using Digimizer software (Figure 4b) to an accuracy of 0.01 mm. Finally, the CAI value is obtained by multiplying the wear flat by 10. To eliminate error, the test was repeated five times for each stone and the arithmetic mean was reported as the CAI (Figure 5). The CAI values of the granite samples are presented in Table 5. The results indicated that CAI values for studied stones range from 3.25 to 4.68. So, they are classified as high and very high abrasive stones according to the classification of CAI proposed by ISRM [6]. Among the stones, ZA has highest abrasivity, while MN and RY showed the least abrasivity.

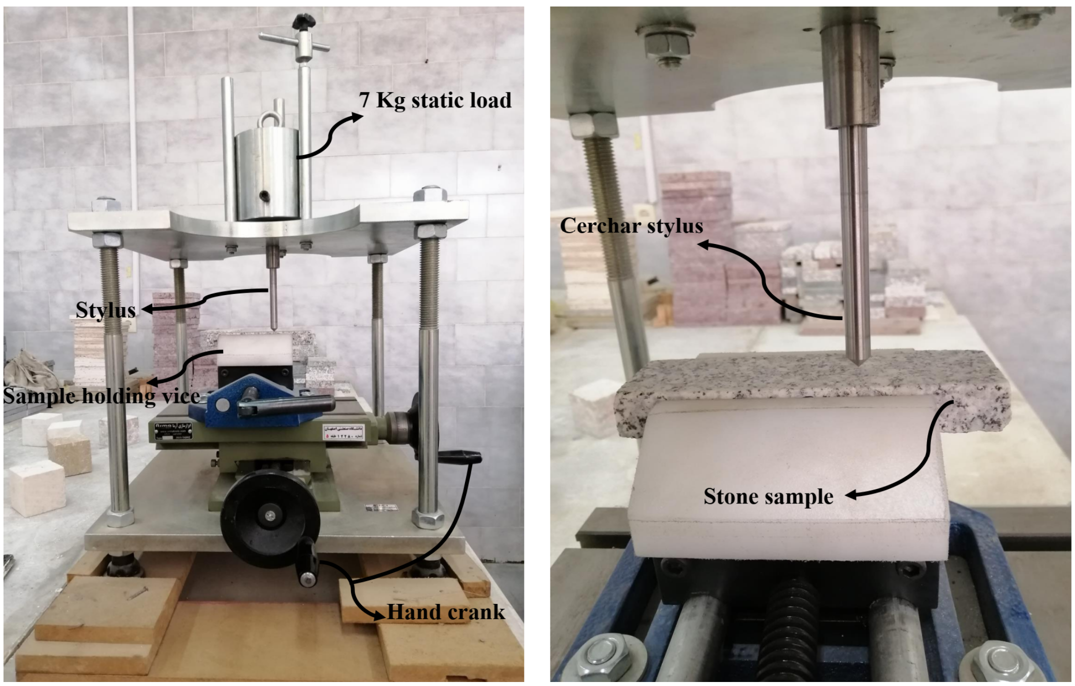

Figure 3. Setup testing device used in this study to measure CAI

(a) (b)

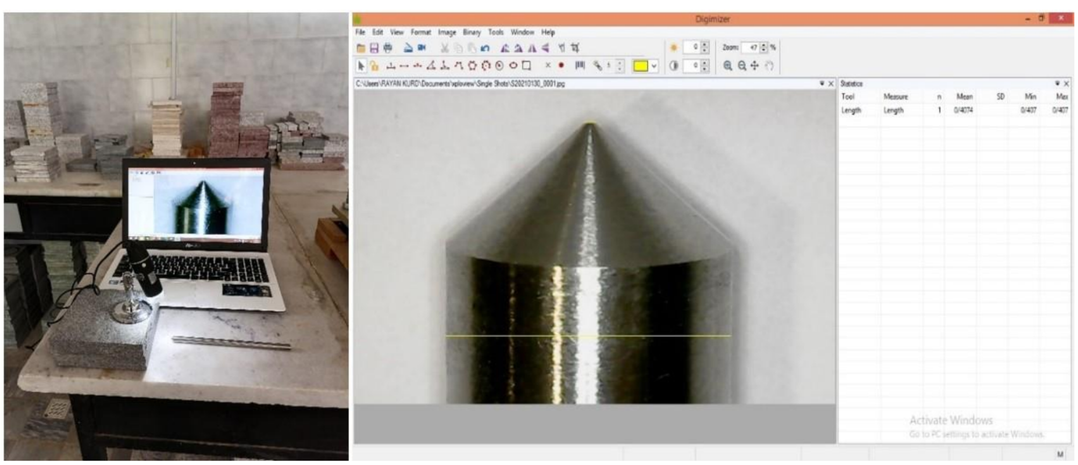

Figure 4. Measurement of wear flat on the steel stylus tip by (a) high-resolution camera, and (b) Digimizer software

2.4. Cutting tests

The cutting tests were performed on all studied stones using circular sawing machine equipped with diamond disc (Figure 6) to determine diamond segment wear (SW). To perform this test, 2 cm thick samples were prepared for all stones, and cutting tests were performed under constant conditions of machine operational parameters for all stones. A constant 3 m cutting length was applied throughout the tests for all stones. Then, the SW was determined for each stone based on weight loss of disc before and after cutting test to an accuracy of 0.001 gr. This test was repeated three times for each sample, and the mean values were considered as SW in this study. The SW values obtained for each stone are presented in last column of Table 5. As can be seen, the highest value of SW is related to the ZA stone, and the lowest value is related to the HZ stone.

Figure 5. Scratched appearance of stone sample after five tests

Figure 6. A view of circular sawing machine used in this study to measure SW

3. Relationship between CAI and stone properties

This section investigates the relationship of CAI with the physico-mechanical and petrographic properties of studied stones. For this purpose, SRA and MRA have been used in SPSS software [45].

3.1. Simple regression analysis (SRA)

The SRA provides a means of summarizing the relationship between two variables [46–50]. The relationships between CAI and the other parameters were analyzed employing power, linear, exponential, and logarithmic functions. During SRA implementation, the CAI was assumed to be the dependent variable and Q/CLV, MH, EQC, Gs, Vp, SCH, BTS, UCS, P, and D were considered as independent variables. The analysis of variance (ANOVA) is used to identify the best possible relation between variables. In the ANOVA test, coefficient of determination (R^2), Fisher-test constant (F-value), and statistical significance (Sig.) indexes are applied for selecting the best correlation. The statistically significant and strong correlations, with the lowest Sig. value and the highest R^2 and F values, were then selected and the regression equation was established among the independent variables with the CAI.

Table 6 presents the details of obtained results. Figures 7 and 8 show the relationship between CAI with petrographic and physico-mechanical properties, respectively. As can be seen, all independent variables have a meaningful relationship with CAI in the confidence interval of 5% (Sig. value ≤ 0.05) except for P and D. Since the variation range for P and D of samples was narrow, no meaningful relationship between these variables and CAI was observed. The results indicate that for Gs, Q/CLV, UCS, Vp, and SCH, the linear function presents the best correlation with R^2 of 0.464, 0.786, 0.481, 0.453 and 0.353, respectively. While, for BTS and MH, the exponential function represents the best correlation with R^2 of 0.476 and 0.543, respectively.

Furthermore, for EQC the power function represents the best correlation with R^2 of 0.882. Among independent variables, petrographic properties have more significant correlations with CAI than the physico-mechanical properties. According to Table 6, EQC, Q/CLV, and MH are the first three stone properties that affect CAI. As can be seen in Figures 7 and 8, CAI increases by increasing Gs, Q/CLV, MH, EQC, Vp, SCH, BTS and UCS. Q/CLV, MH, EQC, Vp, SCH, and stone strength (BTS and UCS) show the stone resistance to permanent deformation [27,38,51]. In other words, increasing these properties lead to increase of stone resistance to deformation. Therefore, increasing these properties result in more severe wear flat of steel stylus tip during Cerchar abrasivity test, means that the stone abrasivity (CAI) increases. It should be noted that the direct linear relationship between the Q/CLV and CAI implies that cleavable minerals lead to decrease of SA. Cleavable minerals have cleavage planes, where the minerals are split and separated easily from the stone along definite planes of weak bonding [20,37]. Therefore, presence of cleavable minerals has detrimental effects on the stone abrasivity. Furthermore, the results indicate that increasing Gs lead to increase of abrasivity. It can be attributed to the increased abrasive effect of the minerals (especially quartz) due to their higher surface area [52]. The direct relationship between SA and mentioned stone properties is in accordance with the literature findings [13,20,33,53,54].

Table 6. Summary of obtained results from SRA

Independent variable	Best fit model	Correlation	F-value	Sig.	R^2
Q/CLV	Liner	$CAI = 1.537 \times (Q/CLV) + 3.263$	44.122	0.000	0.786
Gs	Liner	$CAI = 0.282 \times Gs + 3.315$	10.409	0.007	0.464
EQC	Power	$CAI = 0.288 \times EQC^{0.666}$	89.324	0.000	0.882
MH	Exponential	$CAI = 0.425\exp(0.371 \times MH)$	14.274	0.003	0.543
UCS	Liner	$CAI = 0.027 \times UCS + 0.138$	11.133	0.006	0.481
BTS	Exponential	$CAI = 2.109\exp(0.056 \times BTS)$	10.917	0.006	0.476
Vp	Liner	$CAI = 0.001 \times Vp + 0.921$	9.932	0.008	0.453
SCH	Liner	$CAI = 0.049 \times SCH + 0.722$	6.541	0.025	0.353
D	Liner	$CAI = -0.189 \times D + 4.347$	0.032	0.861	0.003
P	Exponential	$CAI = 4.071\exp(-0.043 \times P)$	0.905	0.360	0.070

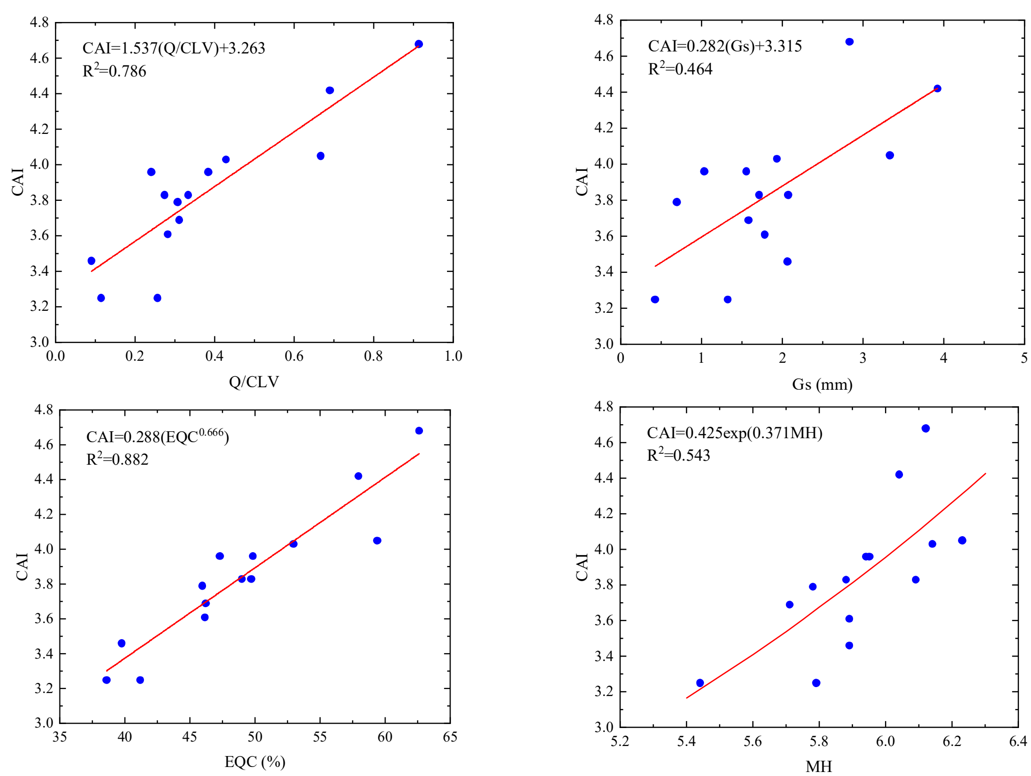

Figure 7. Relationship between CAI and petrographic properties

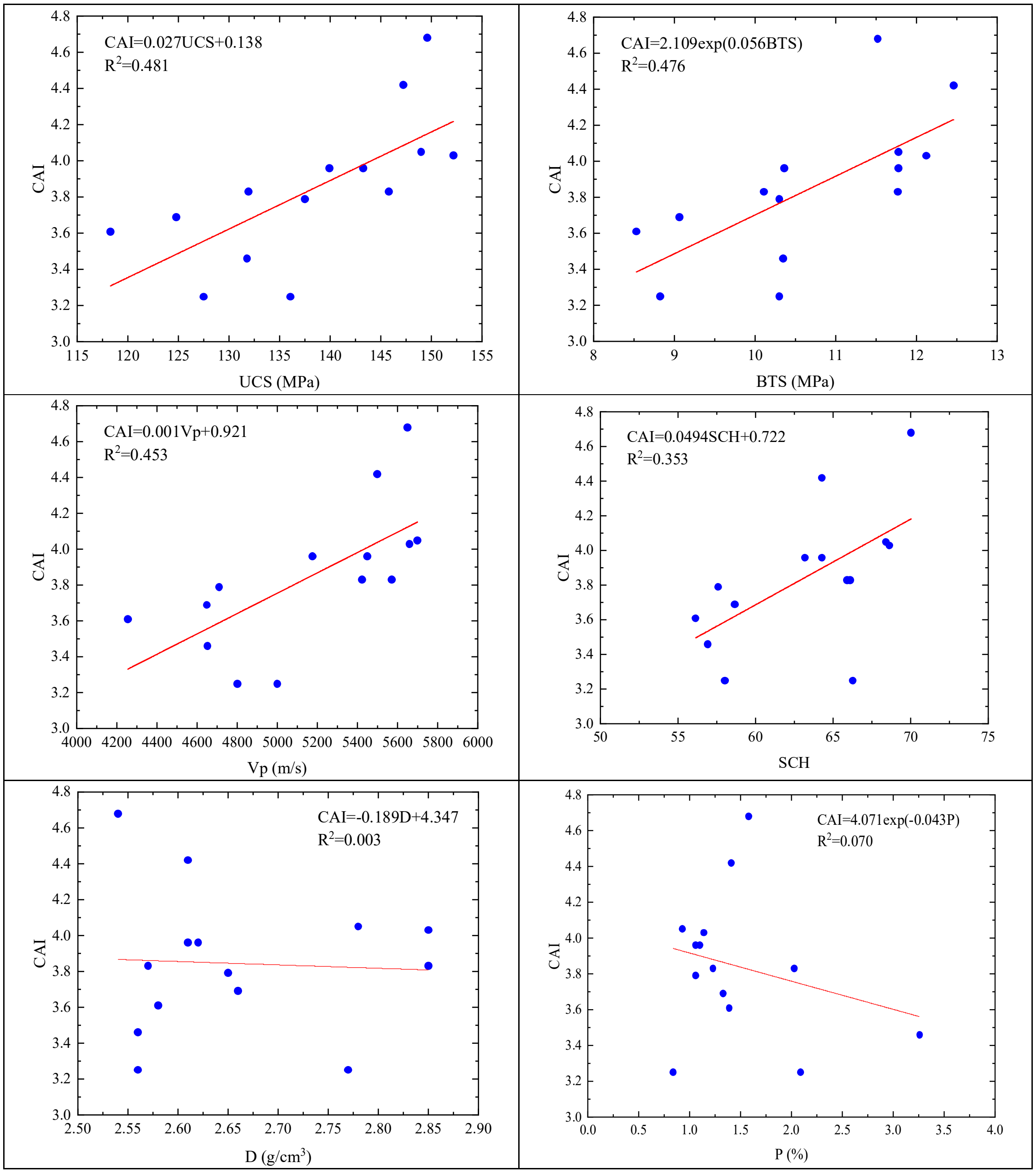

Figure 8. Relationship between CAI and physico-mechanical properties

3.2. Multiple regression analysis (MRA)

The main purpose of multiple regression is to learn more about the linear and nonlinear relationship between several predictor (independent) variables and a dependent variable [46]. In fact, this section aims to investigate the relationship between CAI with Q/CLV, Gs, EQC, MH, Vp, SCH, UCS, and BTS using MRA. One of the strict conditions for MRA is that all predictor variables should be independent. Figure 9 shows the Pearson correlation between the predictor variables in this study. As can be seen, the predictor variables have very high correlation. In these conditions, multicollinearity problem occurs during MRA [55–58]. Multicollinearity occurs when predictor variables in a regression model are correlated. Multicollinearity will lead to less reliable statistical results, depending on the degree of correlation between the predictor variables. One problem derived from multicollinearity is that regression coefficients obtained from the MRA may not compatible with intuition based on past experience and engineering judgment. To solve this issue, the stepwise method can be used in SPSS software to develop a regression model [57].

Stepwise regression is the step-by-step iterative construction of a regression model that involves the selection of predictor variables to be used in a final model. It involves adding or removing potential predictor variables in succession and testing for statistical significance after each iteration. The stepwise regression method takes into account the correlation between the parameters, selects the most effective input variables to develop the model, and removes the other (ineffective) variables.

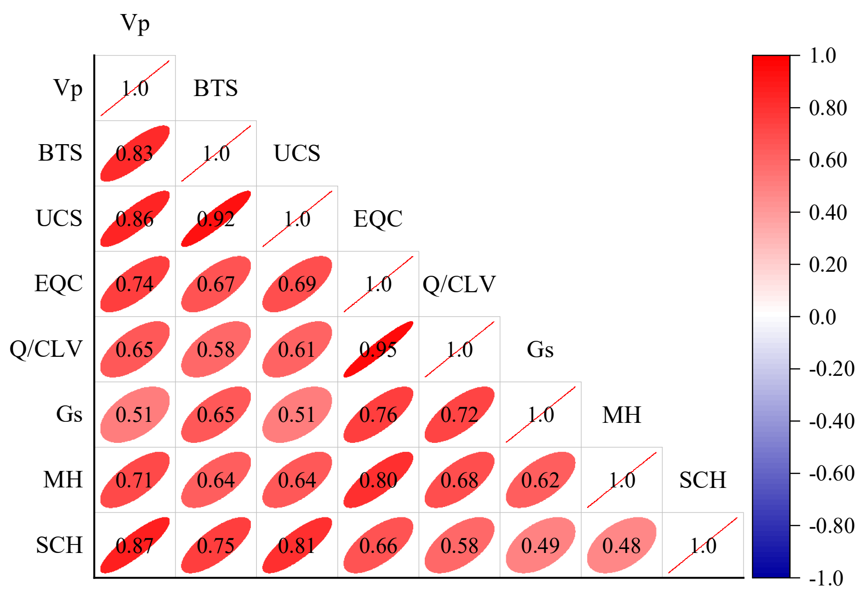

Figure 9. Pearson correlation between stone properties

In this study, the EQC was selected as the main parameter determining the CAI after applying the stepwise regression method. Therefore, two correlations were developed to predict the CAI based on linear and nonlinear regression analysis according to Equations 4 and 5, respectively:

$$CAI = (0.052 \times EQC) + 1.299 \tag{4}$$

$$CAI = 0.288 \times EQC^{0.666} \tag{5}$$

In the following, the accuracy of proposed correlations was evaluated based on six statistical indices, namely R^2, mean absolute error (MAE), root mean square error (RMSE), variance account for (VAF), Nash-Sutcliffe efficiency (NSE), and performance index (PI). The relationship between the actual CAI values and those predicted by Equations 4 and 5 are shown in Figure 10. As can be seen, the R^2 values for developed linear and nonlinear correlations were obtained 0.876 and 0.882, respectively. The RMSE, MAE, VAF, NSE, and PI were calculated using Equations 6 to 10, respectively [32,59–61]. Theoretically, a predictive correlation is excellent when R^2 and NSE are 1, RMSE and MAE are 0, VAF is 100%, and PI is 2.

$$RMSE = \sqrt{\frac{1}{N}\sum_{i=1}^{n}(A_i - P_i)^2} \tag{6}$$

$$MAE = \frac{\sum_{i=1}^{N}|P_i - A_i|}{N} \tag{7}$$

$$VAF = \left[1 - \frac{var(A_i - P_i)}{var(A_i)}\right] \times 100 \tag{8}$$

$$NSE = 1 - \frac{\sum_{i=1}^{N}(P_i - A_i)^2}{\sum_{i=1}^{N}(A_i - A_{avg})^2} \tag{9}$$

$$PI = (R^2 + (\frac{VAF}{100}) - RMSE) \tag{10}$$

Where are:

A_i and P_i- measured and predicted values of CAI,

A_{avg} - the average of measured values for CAI,

N - the number of stone samples.

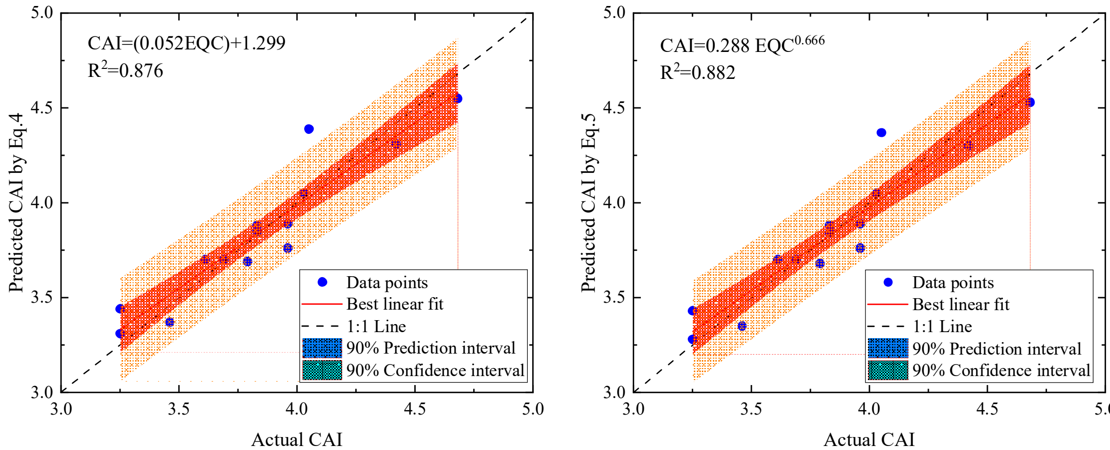

Figure 10. Relationship between actual and predicted CAI values by (a) Equation 4, and (b) Equation 5

Table 7 presents the comparison of predicted CAI values using the linear and nonlinear correlations and actual CAI values. The values of R^2, RMSE, MAE, VAF, NSE and PI for proposed correlations are given in Table 8. These indices illustrate that the proposed correlations are very similar in performance. Both correlations have good prediction capacity and predict CAI with acceptable accuracy. According to the obtained values, it is concluded that the nonlinear correlation is just a little more accurate than the linear correlation.

Table 7. Comparison of predicted and measured values of CAI and SW

Stone code	CAI			SW (gr)	
	Actual	Predicted by Eq. 4	Predicted by Eq. 5	Actual	Predicted by Eq. 11
MN	3.25	3.31	3.28	0.285	0.222
SN	3.69	3.70	3.70	0.258	0.317
KH	3.83	3.85	3.84	0.264	0.348
GN	3.96	3.89	3.89	0.402	0.376
TY	4.03	4.05	4.05	0.441	0.392
BO	3.61	3.70	3.70	0.300	0.300
ZA	4.68	4.55	4.53	0.535	0.533
RY	3.25	3.44	3.43	0.244	0.222
MO	3.79	3.69	3.68	0.337	0.339
SN	3.96	3.76	3.76	0.396	0.376
TA	4.42	4.31	4.30	0.471	0.477
KP	4.05	4.39	4.37	0.395	0.396
HZ	3.46	3.37	3.35	0.192	0.267
MA	3.83	3.88	3.88	0.396	0.348

Table 8. The values of statistical indices for developed correlations

Output	Correlation	R^2	RMSE	MAE	VAF	NSE	PI
CAI	Eq. 4	0.876	0.135	0.105	87.615	0.876	1.617
	Eq. 5	0.882	0.135	0.105	87.748	0.877	1.624
SW	Eq. 11	0.787	0.044	0.033	78.705	0.787	1.530

4. Relationship between SW and CAI

For decades, the Cercahr abrasivity test has been used for estimation of the tool wear or lifetime in various mining and tunneling applications. Furthermore, several empirical correlations have been established between tool consumption (wear) and CAI or a combination of CAI with other rock mechanical parameters like UCS [3,27,62–71]. The circular sawing machines are one of the most common machines used in the stone processing plants to cut stones into different sizes. These machines are widely used because they are fast, economical, flexible, and easy to operate [72]. In these machines, the diamond segments welded on circular steel disc are used to cut stones. During the cutting process, mechanical interaction between diamond segment and stone results in diamond segment wear (SW). SW decreases the cutting rate and increases the cutting energy. So, it is a major factor in determining the cutting duration, the disc lifetime and the cost of cutting. SA has a significant impact on SW [73]. Despite the importance of SW in cutting of granitic building stones, very limited work has been conducted to develop practical correlations for predicting SW based on CAI.

The following investigated the relationship between SW (obtained from cutting tests) and CAI for the studied stones. To examine the relationship between the SW and CAI, SRA were performed based on linear, power, exponential, and logarithmic functions. SW and CAI were considered as dependent and independent variables, respectively. As can be seen in Figure 11, the linear function represents the best correlation with R^2 of 0.787, which reflects the strong relationship between these two parameters. The correlation between SW and CAI is expressed as:

$$\mathrm{SW} = 0.218\mathrm{CAI} - 0.487 \quad (11)$$

The comparison of predicted and measured values of SW is shown in Table 7. The RMSE, MAE, VAF, NSE, and PI indices were obtained as 0.044, 0.033, 78.705, 0.787, and 1.530 for Eq. 11, respectively (see Table 8). Therefore, using Equation 11, SW can be predicted with high accuracy (in gr). This equation is statistically significant in the confidence interval of 1% (Sig. level value ≤ 0.01). Furthermore, a reasonable linearly increasing trend was observed between SW and CAI.

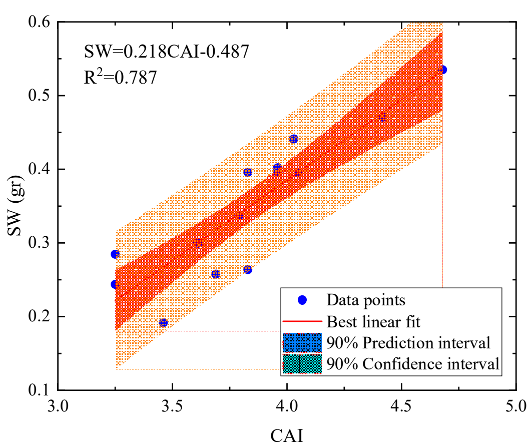

Figure 11. The linear relationship between the SW and CAI

5. Results and discussion

Abrasivity of stones, especially granitic building stones, has a significant role in the consumption (wear) of cutting tools in quarrying and processing of building stones, which affects the cost and duration of operations. One of the most commonly used methods for estimating the stone abrasivity is CAI. Despite the widespread application of this index in the field of mechanized excavation, few studies have been conducted on the application of this index in the building stone industry. Therefore, in this study, the relationship between CAI and petrographic and physico-mechanical properties (including Q/CLV, EQC, Gs, MH, P, D, BTS, UCS, Vp, and SCH) of 14 different Iranian granitic stones were investigated using SRA and MRA techniques. Based on SRA, all stone properties have reasonable and meaningful relationship with CAI except for P and D) owing to their limited variation ranges. Among stone properties, petrographic properties have more significant correlations with CAI than the physico-mechanical properties and EQC, Q/CLV, and MH are the first three stone properties that affect the CAI. The results showed that CAI has a tendency to increase with increasing Q/CLV, Gs, EQC, MH, UCS, BTS, Vp, and SCH, indicating enhanced stone resistance to deformation, hence increasing wear on the steel stylus during the Cerchar test. The existence of cleavable minerals, including plagioclase and K-feldspar, was seen to diminish stone abrasivity owing to their weak bonding planes. Moreover, higher grain sizes enhanced abrasivity, mostly due to the augmented surface area of quartz, in accordance with existing research.

The MRA was performed using stepwise regression method to eliminate the multicollinearity problem due to high correlation between the stone properties. Based on stepwise regression method, the EQC was selected as the main parameter for determining the CAI and two new empirical correlations have been developed to predict the CAI: a linear model (R^2 = 0.876) and a nonlinear model (R^2 = 0.882), both exhibiting substantial predictive precision. The significant impact of EQC on CAI is due to its representation of the abrasive capacity of minerals in the stone, adjusted for their Rosiwal hardness in comparison to quartz, the hardest and most abrasive mineral found in granitic stones. Quartz dominates in the wear process owing to its scratch resistance and its capacity to cause substantial wear on the steel stylus during the Cerchar test. EQC amalgamates the contributions of all minerals (e.g., quartz, K-feldspar, plagioclase) by multiplying their percentage composition by their corresponding hardness values, yielding a holistic assessment of the stone's abrasivity. This explains the high R^2 observed in the power function relationship, as EQC effectively captures the combined influence of mineral hardness and content, unlike singular indices such as Q or MH. These correlations improve upon previous models, such as those by Er and Tuğrul, which reported lower R^2 values (0.5–0.8) for granitic rocks [21], due to the targeted selection of EQC and the use of a robust dataset specific to granitic building stones.

6. Limitations and future studies

This study offers substantial insights into the correlation between the Cerchar Abrasivity Index (CAI) and the petrographic and physico-mechanical properties of granitic building stones, along with the relationship between CAI and diamond segment wear (SW), yet it is constrained by specific limitations. The work used a dataset of 14 commercial granitic stones obtained solely from Iran, potentially constraining the applicability of the postulated empirical correlations to other geological contexts or stone varieties with distinct mineralogical and mechanical properties. Secondly, the laboratory experiments were performed under controlled conditions, including a fixed cutting length of 3 meters and defined operational parameters for the circular sawing machine, which may not entirely reflect the actual industrial environments. The study largely emphasized equivalent quartz content (EQC) as the principal parameter for CAI prediction, possibly neglecting the cumulative impacts of other petrographic or mechanical parameters due to multicollinearity, which was addressed using stepwise regression. The Cerchar abrasivity test, however extensively utilized, may be affected by factors such as the precision of stylus wear assessment and differences in surface conditions, potentially leading to slight discrepancies in CAI findings.

Future research should broaden the dataset to include a wider variety of granitic and non-granitic stones from diverse geological locations to enhance the applicability of the predictive models. Examining the synergistic effects of various petrographic and physico-mechanical properties using advanced statistical or machine learning techniques (such as principle component analysis or random forest) may improve predictive accuracy and more effectively address multicollinearity. Additionally, conducting cutting experiments under varied operating conditions (e.g., different cutting speeds, depths, or machine types) would provide a more comprehensive understanding of sawability behavior in industrial applications. Investigating the influence of environmental factors, such as stone moisture content and temperature, on CAI and SW could further refine the models. Ultimately, integrating the proposed correlations into real-time monitoring systems for stone processing facilities merits exploration to validate their practical utility and support the automated optimization of cutting processes.

7. Conclusion

This study established new empirical correlations for predicting the Cerchar Abrasivity Index (CAI) and diamond segment wear (SW) of granitic building stones, filling a significant void in the building stone sector. Employing 14 granitic stones, the linear and nonlinear correlations for CAI prediction based on EQC. The prediction performances of both developed correlations were evaluated using six statistical indices: R^2, RMSE, MAE, VAF, NSE, and PI. For the linear correlation, the R^2, VAF, RMSE, MAE, NSE, and PI were equal to 0.876, 0.135, 0.105, 87.615, 0.876, and 1.617, respectively. For the non-linear correlation, the R2, VAF, RMSE, NSE, MAE, and PI were obtained as 0.882, 0.135, 0.105, 0.877, 87.748, and 1.624, respectively. These values indicated that both correlations have good prediction capacity and predict the CAI with acceptable accuracy, but the nonlinear correlation is a little more accurate than the linear correlation.

Finally, the relationship between SW and CAI for the studied stones was investigated. The results indicated that there is a strong linear correlation between SW and CAI with a R^2 of 0.787. The proposed correlation can be applied for fast prediction of SW with acceptable error for practical applications in building stone processing plants with circular sawing machine. It can be used for primary estimation of cutting duration, the disc lifetime and the cost of cutting.

References

[1]. Farhadian, A., Ghasemi, E., Hoseinie, S.H., & Bagherpour, R. (2022). Prediction of rock abrasivity index (RAI) and uniaxial compressive strength (UCS) of granite building stones using nondestructive tests. *Geotechnical and Geological Engineering*, 40(8), 3343–3356.

[2]. Plinninger, R.J., & Restner, U. (2008). Abrasiveness testing, quo vadis? – A commented overview of abrasiveness testing methods. *Geomechanics and Tunnelling*, 1(1), 61–70.

[3]. Ko, T.Y., Kim, T.K., Son, Y., & Jeon, S. (2016). Effect of geomechanical properties on Cerchar abrasivity index (CAI) and its application to TBM tunnelling. *Tunnelling and Underground Space Technology*, 57, 99–111.

[4]. Rostami, J., Ghasemi, A., Gharahbagh, E.A., Dogruoz, C., & Dahl, F. (2014). Study of dominant factors affecting Cerchar abrasivity index. *Rock Mechanics and Rock Engineering*, 47(5), 1905–1919.

[5]. Alber, M., Yaralı, O., Dahl, F., Bruland, A., Käsling, H., & Michalakopoulos, T.N. (2013). ISRM suggested method for determining the abrasivity of rock by the Cerchar abrasivity test. In: *The ISRM Suggested Methods for Rock Characterization, Testing and Monitoring: 2007–2014*. Cham: Springer International Publishing, 101–106.

[6]. Alber, M., Yaralı, O., Dahl, F., Bruland, A., Käsling, H., & Michalakopoulos, T.N. (2014). ISRM suggested method for determining the abrasivity of rock by the Cerchar abrasivity test. *Rock Mechanics and Rock Engineering*, 47(1), 261–266.

[7]. Plinninger, R., Käsling, H., Thuro, K., & Spaun, G. (2003). Testing conditions and geomechanical properties influencing the Cerchar abrasiveness index (CAI) value. *International Journal of Rock Mechanics and Mining Sciences*, 40(2), 259–263.

[8]. Suana, M., & Peters, T. (1982). The Cerchar abrasivity index and its relation to rock mineralogy and petrography. *Rock Mechanics*, 15(1), 1–8.

[9]. West, G. (1989). Rock abrasiveness testing for tunnelling. *International Journal of Rock Mechanics and Mining Sciences & Geomechanics Abstracts*, 26(2), 151–160.

[10]. Al-Ameen, S.I., & Waller, M.D. (1994). The influence of rock strength and abrasive mineral content on the Cerchar abrasive index. *Engineering Geology*, 36(3–4), 293–301.

[11]. Lassnig, K., Latal, C., & Klima, K. (2008). Impact of grain size on the Cerchar abrasiveness test. *Geomechanics and Tunnelling*, 1(1), 71–76.

[12]. Yaralı, O., Yaşar, E., Bacak, G., & Ranjith, P.G. (2008). A study of rock abrasivity and tool wear in coal measures rocks. *International Journal of Coal Geology*, 74(1), 53–66.

[13]. Khandelwal, M., & Ranjith, P.G. (2010). Correlating index properties of rocks with P-wave measurements. *Journal of Applied Geophysics*, 71(1), 1–5.

[14]. Altindag, R., Sengun, N., Sarac, S., Mutluturk, M., & Guney, A. (2009). Evaluating the relations between brittleness and Cerchar abrasion index of rocks. In: *ISRM Regional Symposium - EUROCK 2009*, ISRM-EUROCK-2009-028.

[15]. Kahraman, S., Alber, M., Fener, M., & Gunaydin, O. (2010). The usability of Cerchar abrasivity index for the prediction of UCS and E of Misis fault breccia: Regression and artificial neural networks analysis. *Expert Systems with Applications*, 37(12), 8750–8756.

[16]. Dipova, N. (2012). Investigation of the relationships between abrasiveness and strength properties of weak limestone along a tunnel route. *Geological Engineering*, 36(1), 23–34.

[17]. Deliormanlı, A.H. (2012). Cerchar abrasivity index (CAI) and its relation to strength and abrasion test methods for marble stones. *Construction and Building Materials*, 30, 16–21.

[18]. Tripathy, A., Singh, T.N., & Kundu, J. (2015). Prediction of abrasiveness index of some Indian rocks using soft computing methods. *Measurement*, 68, 302–309.

[19]. Er, S., & Tuğrul, A. (2016). Estimation of Cerchar abrasivity index of granitic rocks in Turkey by geological properties using regression analysis. *Bulletin of Engineering Geology and the Environment*, 75(3), 1325–1339.

[20]. Er, S., & Tuğrul, A. (2016). Correlation of physico-mechanical properties of granitic rocks with Cerchar abrasivity index in Turkey. *Measurement*, 91, 114–123.

[21]. He, J., Li, S., Li, X., Wang, X., & Guo, J. (2016). Study on the correlations between abrasiveness and mechanical properties of rocks combining with the microstructure characteristic. *Rock Mechanics and Rock Engineering*, 49(7), 2945–2951.

[22]. Majeed, Y., & Bakar, M.Z.A. (2016). Statistical evaluation of Cerchar abrasivity index (CAI) measurement methods and dependence on petrographic and mechanical properties of selected rocks of Pakistan. *Bulletin of Engineering Geology and the Environment*, 75(3), 1341–1360.

[23]. Moradizadeh, M., Cheshomi, A., Ghafoori, M., & Tarigh Azali, S. (2016). Correlation of equivalent quartz content, slake durability index and Is50 with Cerchar abrasiveness index for different types of rock. *International Journal of Rock Mechanics and Mining Sciences*, 86, 67–75.

[24]. Bakar, M.Z.A., Majeed, Y., & Rostami, J. (2016). Effects of rock water content on Cerchar abrasivity index. *Wear*, 368–369, 132–145.

[25]. Ündül, Ö., & Er, S. (2017). Investigating the effects of micro-texture and geo-mechanical properties on the abrasiveness of volcanic rocks. *Engineering Geology*, 229, 85–94.

[26]. Capik, M., & Yilmaz, A.O. (2017). Correlation between Cerchar abrasivity index, rock properties, and drill bit lifetime. *Arabian Journal of Geosciences*, 10(1), 15.

[27]. Cheshomi, A., & Moradhaseli, S. (2017). Effect of petrographic characteristics on abrasive properties of granitic building stones. *Quarterly Journal of Engineering Geology and Hydrogeology*, 50(3), 347–353.

[28]. Ozdogan, M.V., Deliormanlı, A.H., & Yenice, H. (2018). The correlations between the Cerchar abrasivity index and the geomechanical properties of building stones. *Arabian Journal of Geosciences*, 11(9), 1–13.

[29]. Torrijo, F.J., Garzón-Roca, J., Company, J., & Cobos, G. (2019). Estimation of Cerchar abrasivity index of andesitic rocks in Ecuador from chemical compounds and petrographical properties using regression analyses. *Bulletin of Engineering Geology and the Environment*, 78(4), 2331–2344.

[30]. Erarslan, N. (2019). Assessment of Cerchar abrasivity test in anisotropic rocks. *Geomechanics and Engineering*, 17(6), 527–534.

[31]. Kadkhodaei, M.H., & Ghasemi, E. (2019). Development of a GEP model to assess Cerchar abrasivity index of rocks based on geomechanical properties. *Journal of Mining and Environment*, 10(4), 917–928.

[32]. Teymen, A. (2020). The usability of Cerchar abrasivity index for the estimation of mechanical rock properties. *International Journal of Rock Mechanics and Mining Sciences*, 128, 104258.

[33]. Garzón-Roca, J., Torrijo, F.J., Alonso-Pandavenes, O., & Alija, S. (2020). Cerchar abrasivity index estimation of andesitic rocks in Ecuador from petrographical properties using artificial neural networks. *International Journal of Geomechanics*, 20(4), 04020036.

[34]. Zhang, S.R., She, L., Wang, C., Wang, Y.J., Cao, R.L., & Li, Y.L. (2021). Investigation on the relationship among the Cerchar abrasivity index, drilling parameters and physical and mechanical properties of the rock. *Tunnelling and Underground Space Technology*, 112, 103907.

[35]. Kwak, N., & Ko, T. (2022). Machine learning-based regression analysis for estimating Cerchar abrasivity index. *Geomechanics and Engineering*, 29(3), 219–228.

[36]. Yılmaz, N.G., Goktan, R.M., & Onargan, T. (2017). Correlative relations between three-body abrasion wear resistance and petrographic properties of selected granites used as floor coverings. *Wear*, 372–373, 197–207.

[37]. Farhadian, A., Ghasemi, E., Hoseinie, S.H., & Bagherpour, R. (2021). Development of a new test method for evaluating the abrasivity of granite building stones during polishing process based on weight loss of abrasive tool. *Construction and Building Materials*, 303, 124497.

[38]. Sousa, L.M.O. (2013). The influence of the characteristics of quartz and mineral deterioration on the strength of granitic dimensional stones. *Environmental Earth Sciences*, 69(4), 1333–1346.

[39]. Thuro, K. (1997). Drillability prediction: Geological influences in hard rock drill and blast tunnelling. *Geologische Rundschau*, 86(2), 426–438.

[40]. Yilmaz, N.G. (2011). Abrasivity assessment of granitic building stones in relation to diamond tool wear rate using mineralogy-based rock hardness indexes. *Rock Mechanics and Rock Engineering*, 44(6), 725–733.

[41]. Brown, E.T. (1981). Rock characterization, testing & monitoring: ISRM suggested methods. Oxford: Pergamon Press.

[42]. ASTM C170. (2017). Standard test method for compressive strength of dimension stone. *ASTM International*.

[43]. Aydin, A. (2008). ISRM suggested method for determination of the Schmidt hammer rebound hardness: Revised version. In: *The ISRM Suggested Methods for Rock Characterization, Testing and Monitoring: 2007–2014*. Cham: Springer International Publishing, 25–33.

[44]. SPSS16.0. (2007). Statistical analysis software (Standard Version). SPSS Inc.

[45]. Sari, M., Ghasemi, E., & Ataei, M. (2014). Stochastic modeling approach for the evaluation of backbreak due to blasting operations in open pit mines. *Rock Mechanics and Rock Engineering*, 47(2), 771–783.

[46]. Rezaei, M., & Esmaeili, K. (2024). The anisotropy of rock drilling in marble quarry mining based on the relationship between vertical and horizontal drilling rates. *International Journal of Geomechanics*, 24(10), 04024236.

[47]. Rezaei, M., & Nyazyan, N. (2023). Assessment of effect of rock properties on horizontal drilling rate in marble quarry mining: Field and experimental studies. *Journal of Mining and Environment*, 14(1), 321–339.

[48]. Rezaei, M., & Esmaeili, K. (2024). The anisotropy of rock drilling in marble quarry mining based on the relationship between vertical and horizontal drilling rates. *Journal of Geotechnical and Geoenvironmental Engineering*, 24(1), 1–13.

[49]. Rezaei, M., Koureh Davoodi, P., & Najmoddini, I. (2019). Studying the correlation of rock properties with P-wave velocity index in dry and saturated conditions. *Journal of Applied Geophysics*, 169, 49–57.

[50]. Petrica, M., Badisch, E., & Peinsitt, T. (2013). Abrasive wear mechanisms and their relation to rock properties. *Wear*, *308*(1–2), 86–94.

[51]. Deliormanlı, A.H. (2012). Cerchar abrasivity index (CAI) and its relation to strength and abrasion test methods for marble stones. *Construction and Building Materials*, 30, 16–21.

[52]. Ündül, Ö., & Er, S. (2017). Investigating the effects of micro-texture and geo-mechanical properties on the abrasiveness of volcanic rocks. *Engineering Geology*, 229, 85–94.

[53]. Farrar, D.E., & Glauber, R.R. (1967). Multicollinearity in regression analysis: The problem revisited. *Review of Economics and Statistics*, 49(1), 92–107.

[54]. Montgomery, D., Peck, E., & Vining, G. (2012). Multicollinearity diagnostics. In: *Introduction to Linear Regression Analysis*. *Wiley,* 292–302.

[55]. Bahri, M., Ghasemi, E., Kadkhodaei, M.H., Romero-Hernández, R., & Mascort-Albea, E.J. (2021). Analysing the life index of diamond cutting tools for marble building stones based on laboratory and field investigations. *Bulletin of Engineering Geology and the Environment*, 80(10), 7959–7971.

[56]. Shrestha, N. (2020). Detecting multicollinearity in regression analysis. *American Journal of Applied Mathematics and Statistics*, 8(2), 39–42.

[57]. Azimian, A. (2017). Application of statistical methods for predicting uniaxial compressive strength of limestone rocks using nondestructive tests. *Acta Geotechnica*, 12(2), 321–333.

[58]. Kong, F., Xue, Y., Qiu, D., Gong, H., & Ning, Z. (2021). Effect of grain size or anisotropy on the correlation between uniaxial compressive strength and Schmidt hammer test for building stones. *Construction and Building Materials*, 299, 123941.

[59]. Yagiz, S., Sezer, E.A., & Gokceoglu, C. (2012). Artificial neural networks and nonlinear regression techniques to assess the influence of slake durability cycles on the prediction of uniaxial compressive strength and modulus of elasticity for carbonate rocks. *International Journal of Numerical and Analytical Methods in Geomechanics*, *36*(14), 1636–1650.

[60]. Maidl, B., Schmid, L., Ritz, W., & Herrenknecht, M. (2008). Hardrock tunnel boring machines. Wiley.

[61]. Dahl, F., Bruland, A., Jakobsen, P.D., Nilsen, B., & Grøv, E. (2012). Classifications of properties influencing the drillability of rocks, based on the NTNU/SINTEF test method. *Tunnelling and Underground Space Technology*, 28, 150–158.

[62]. Gehring, K. (1995). Prognosis of advance rates and wear for underground mechanized excavations. *Felsbau*, 13(6), 439–448.

[63]. Bruland, A. (1999). Hard rock tunnel boring – Advance rate and cutter wear. *NTNU/SINTEF Report*, 3.

[64]. Plinninger, R.J., & Thuro, K. (2004). Wear prediction in hardrock excavation using the Cerchar abrasiveness index (CAI). In: *International Symposium EUROCK 2004*, 1–6.

[65]. Rostami, J., Ozdemir, L., Bruland, A., & Dahl, F. (2005). Review of issues related to Cerchar abrasivity testing and their implications on geotechnical investigations and cutter cost estimates. In: *Proceedings of the Rapid Excavation and Tunneling Conference (RETC)*, 738–751.

[66]. Frenzel, C. (2011). Disc cutter wear phenomenology and their implications on disc cutter consumption for TBM. In: *45th US Rock Mechanics / Geomechanics Symposium*, ARMA-11-211.

[67]. Massalov, T., Yagiz, S., & Rostami, J. (2020). Relationship between key rock properties and Cerchar abrasivity index for estimation of disc cutter wear life in rock tunneling applications. In: *ISRM International Symposium - EUROCK 2020*, ISRM-EUROCK-2020-162.

[68]. Massalov, T., Yagiz, S., & Adoko, A.C. (2022). Application of soft computing techniques to estimate cutter life index using mechanical properties of rocks. *Applied Sciences*, 12(3), 1446.

[69]. Liu, Q., Liu, J., Pan, Y., Zhang, X., Peng, X., & Gong, Q. (2017). A wear rule and cutter life prediction model of a 20-in. TBM cutter for granite: A case study of a water conveyance tunnel in China. *Rock Mechanics and Rock Engineering*, 50(5), 1303–1320.

[70]. Ersoy, A., Buyuksagic, S., & Atici, U. (2005). Wear characteristics of circular diamond saws in the cutting of different hard abrasive rocks. *Wear*, 258(9–10), 1422–1436.

[71]. Rajpurohit, S.S., Sinha, R.K., & Sen, P. (2020). Influence of Cerchar hardness index of hard rock granite on wear of diamond tools. *Materials Today: Proceedings*, 33, 5471–5475.

انجمن مهندسی معدن ایران
نشریه مهندسی معدن و محیط زیست
نشانی نشریه: www.jme.shahroodut.ac.ir
دانشگاه صنعتی شاهرود

بررسی رابطه بین شاخص سایندگی سرشار با خصوصیات فیزیکی-مکانیکی و سنگ‌شناسی سنگ‌های ساختمانی گرانیتی

سینا قوامی[۱]، ابراهیم قاسمی[۱*]، محمد حسین کدخدایی[۱] و علی فرهادیان[۲]

۱. دانشکده مهندسی معدن، دانشگاه صنعتی اصفهان، اصفهان، ایران
۲. گروه معدن، دانشکده فنی، دانشگاه جیرفت، کرمان، ایران

اطلاعات مقاله

تاریخ ارسال: ۲۰۲۵/۰۵/۲۷
تاریخ داوری: ۲۰۲۵/۰۶/۰۱
تاریخ پذیرش: ۲۰۲۵/۰۶/۲۷

DOI: 10.22044/jme.2025.16303.3167

کلمات کلیدی

شاخص سایندگی سرشار (CAI)
سنگ‌های ساختمانی گرانیتی
خصوصیات سنگ‌شناسی
خصوصیات فیزیکی-مکانیکی
سایش سگمنت الماسه (SW)

چکیده

مصرف ابزارهای برش و ساب یکی از پارامترهای اقتصادی حیاتی در فرآیند استخراج و فرآوری سنگ‌های ساختمانی گرانیتی است که به شدت تحت تأثیر خاصیت سایندگی سنگ قرار می‌گیرد. بنابراین، برآورد سایندگی این سنگ‌ها موضوعی بسیار مهم است. روش‌های متعددی برای تعیین سایندگی سنگ وجود دارد. یکی از رایج‌ترین روش‌ها، شاخص سایندگی سرشار (CAI) است. این مطالعه اساساً بر بررسی رابطه بین CAI و خصوصیات سنگ‌شناسی و فیزیکی-مکانیکی سنگ‌های ساختمانی گرانیتی متمرکز است. برای این منظور، ۱۴ نوع مختلف از سنگ‌های ساختمانی گرانیتی تجاری، جمع‌آوری‌شده از مناطق مختلف ایران، تحت بررسی‌های آزمایشگاهی قرار گرفتند و تأثیر خصوصیات سنگ‌شناسی و فیزیکی-مکانیکی این سنگ‌ها بر CAI با استفاده از تحلیل رگرسیون ساده و چندگانه بررسی شد. روابط معنادار و منطقی مشاهده شد. بر اساس نتایج بدست‌آمده، محتوای معادل کوارتز (EQC) سنگ‌های گرانیتی به‌عنوان مؤثرترین پارامتر بر CAI شناسایی شد. با استفاده از تحلیل رگرسیون خطی و غیرخطی، دو رابطه تجربی برای پیش‌بینی CAI بر اساس EQC توسعه یافت. نتایج نشان داد که هر دو رابطه خطی و غیرخطی عملکرد بالایی دارند و ضرایب تعیین (R^2) به‌ترتیب ۰.۸۷۶ و ۰.۸۸۲ را نشان می‌دهند. این روابط می‌توانند CAI را با خطای قابل‌قبول، با مقادیر ریشه میانگین مربعات خطا (RMSE) و میانگین خطای مطلق (MAE) به‌ترتیب برابر با ۰.۱۳۵ و ۰.۱۰۵، تعیین کنند. علاوه بر این، رابطه بین سایش سگمنت الماسه (SW) و CAI برای سنگ‌های مورد مطالعه بررسی شد. نتایج نشان داد که SW به‌طور مستقیم با CAI مرتبط است و یک رابطه خطی قوی بین این دو پارامتر با R^2 برابر ۰.۷۸۷ وجود دارد. رابطه پیشنهادی می‌تواند به منظور پیش‌بینی سریع سایش ابزار برش برای کاربردهای عملی در کارخانه‌های فرآوری سنگ ساختمانی با دستگاه‌های برش مدور استفاده شود، که این امر می‌تواند منجر به افزایش راندمان برش و بهره‌وری شود.

نویسنده مسئول مکاتبات: *e_ghasemi@iut.ac.ir* (ا. اقاسمی)